Proceedings of the European Conference Physics of Magnetism, Poznań 2017

Influence of Valence Band Modifications on Hydrogen Absorption in Zr-Pd Alloy Thin Films

B. Jabłoński[a,b,*], S. Pacanowski[a], M. Werwiński[a], A. Marczyńska[a], H. Dawczak-Dębicki[a,c], A. Szajek[a], and L. Smardz[a]

[a]Institute of Molecular Physics, Polish Academy of Sciences, M. Smoluchowskiego 17 , 60-179 Poznań, Poland
[b]Faculty of Technical Physics, Poznań University of Technology, Piotrowo 3, 60-965 Poznań, Poland
[c]Faculty of Physics, Adam Mickiewicz University, Umultowska 85, 61-614 Poznań, Poland

We study the valence band modifications of *in-situ* prepared nano- and polycrystalline Pd-Zr alloy thin films using X-ray photoelectron spectroscopy. Results were compared with valence bands calculated by *ab initio* methods. Furthermore, hydrogen absorption and desorption kinetics under pressure of about 570 mbar were studied in Pd covered nanocrystalline $ZrPd_2$ alloy thin film. Results showed that modifications of the valence band of the nanocrystalline alloy thin film could significantly influence on hydrogen absorption and desorption process.

DOI: 10.12693/APhysPolA.133.620
PACS/topics: 73.22.–f, 82.80.Pv

1. Introduction

Intermetallic compounds based on hydrogen absorbing elements usually also form stable hydrides. This is, for instance, the case of $PdZr_2$ alloy [1]. However, a similar compound, $ZrPd_2$ does not absorb hydrogen although both compounds have the same crystal structure and satisfy the empirical geometrical criteria for hydride formation [1]. Results of *ab initio* calculations performed for $ZrPd_2$ single crystal revealed an unanticipated purely electronic origin [1].

In thin film materials dislocations and vacancies are present in higher density than in bulk material [2]. Even when the grain size is maximized by epitaxial film growth, dislocations are generated during the growth process to adjust for the lattice mismatch between the film and the substrate [3]. The local hydrogen affinity is different for these defects and therefore the materials properties are expected to be influenced by all of the mentioned microstructural components. It was shown in Ref. [4] that the valence bands of bulk nanocrystalline and nanocomposite $LaNi_5$-based materials were broadened compared to those measured for polycrystalline samples. Furthermore, practically all of the mechanically alloyed nanomaterials showed significantly greater discharge capacity [5].

Membrane separations have potential advantages over other approaches to hydrogen purification [6–8]. Permeability calculations were performed for the potential candidates. After systematically examining all Pd-based intermetallics, no material was found to have higher hydrogen permeability than pure Pd. Moreover, it has been found very recently from theoretical calculations that $ZrPd_2$ membrane have also potentially interesting permeability [9, 10]. Therefore, modification of the electronic structure of $ZrPd_2$ films by the tuning of their microstructure could potentially improve hydrogen permeability.

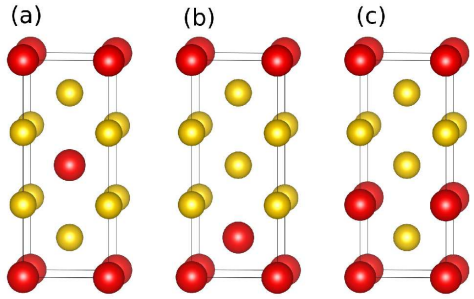

Fig. 1. The considered $ZrPd_2$ models: (a) ordered, (b) Zr-Pd antisites type I, (c) Zr-Pd antisites type II. The bigger red spheres represent Zr, the smaller yellow ones stand for Pd.

In this paper, we study the electronic properties of polycrystalline and nanocrystalline Zr-Pd alloy thin films using X-ray Photoelectron Spectroscopy (XPS) and *ab initio* calculations.

2. Experimental and theoretical methods

The alloy thin films were prepared in the temperature range of 295 K - 700 K using computer-controlled UHV magnetron co-sputtering [11, 12]. Pd and Zr targets were sputtered using DC and RF modes, respectively. The base pressure before the deposition process was lower than 5×10^{-10} mbar. As a substrate we have used Si(100) wafers with an oxidised surface to prevent a silicide formation. Therefore we have applied a special heat treatment in UHV before deposition in order to obtain an epitaxial SiO_2 surface layer [13, 14]. The chemical composition and the cleanness of all layers was

*corresponding author; e-mail: beniamin.jablonski@ifmpan.poznan.pl

checked *in-situ*, immediately after deposition, transferring the samples to an UHV (4×10^{-11} mbar) analysis chamber equipped with XPS. Details of the XPS measurements can be found in Ref. [15–17].

Furthermore, hydrogen absorption and desorption kinetics at room temperature (RT) and at a pressure of about 570 mbar were studied in $ZrPd_2$ (covered by 10 nm – Pd) thin film using four-point resistivity measurements.

The theoretical photoemission spectra are based on the electronic structures calculated with the full-potential linearized augmented-plane wave (FP-LAPW) method implemented in the WIEN2k code [18]. The method of XPS spectra calculations is discussed in more details in our previous work [19]. In this work Perdew-Burke-Ernzerhof form (PBE) [20] of the exchange-correlation potential is selected. The effective on-site Coulomb interactions parameters U(Zr) = 2.4 eV and U(Pd) = 3.7 eV [21] have been taken into account in GGA(PBE)+U scheme. Plane wave cut-off parameter RK_{max} is set to 8, which leads to above 500 basis functions. Relativistic effects are included with the second variational treatment of spin-orbit coupling. The total energy convergence criterion is set to 10^{-8} Ry. 32000 k-points is used in the whole Brillouin zone. Besides the ordered $ZrPd_2$, two simplest models of the disordered structures were considered, see Fig. 1. In these models some Zr and Pd atoms have been exchanged on sites. All three structures have been fully relaxed, which means that the volume, c/a ratio and Wyckoff positions have been optimized. The resultant lattice parameters for ordered structure (a = 0.347 nm and c = 0.8755 nm) are about 1.8% greater than the experimental ones [22], which means a decent agreement. The theoretical XPS for a single crystal with chemical disorder is evaluated as an average of three contributions: an ordered case and two cases with antisites, see Fig. 1.

3. Results and discussion

In Fig. 2 we show XPS core-level spectra of the freshly deposited nanocrystalline $ZrPd_2$ alloy thin film and polycrystalline pure Pd and Zr thin films. The total thickness of the prepared thin films was about 100 nm. Due to well known high reactivity of zirconium with oxygen we have prepared the nanocrystalline alloy thin film after an additional heating of the sample holder and substrate at 700 K for 3 h and cooling to 295 K. Results showed that after such an outgassing procedure, it is possible to prepare oxygen and carbon free Zr, Pd and $ZrPd_2$ surface. In our case, the oxygen and other surface impurities are practically absent on such prepared Zr-based alloy thin films immediately after deposition. As can be seen in Fig. 2, practically no XPS signal from potential contamination atoms like O-1s and C-1s is observed.

Figure 3 shows valence bands of nano- and polycrystalline $ZrPd_2$ alloy thin films. The position of the centroids of the valence bands measured for the two samples with significantly different microstructure are practically

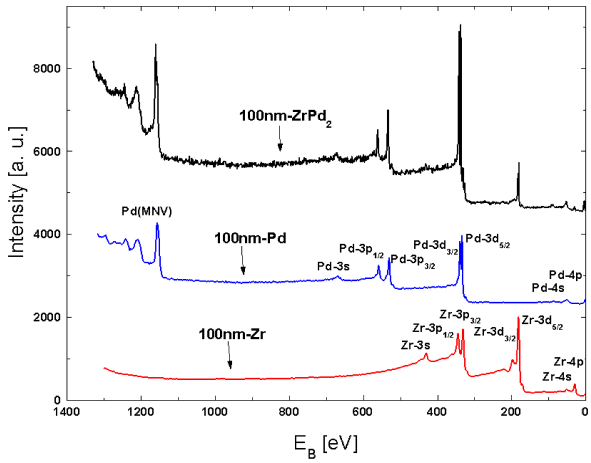

Fig. 2. XPS (Al-K$_\alpha$) spectrum of the freshly prepared polycrystalline $ZrPd_2$ alloy thin film (top curve). For a comparison we also show the XPS spectra measured for *in-situ* prepared polycrystalline Pd and Zr thin films.

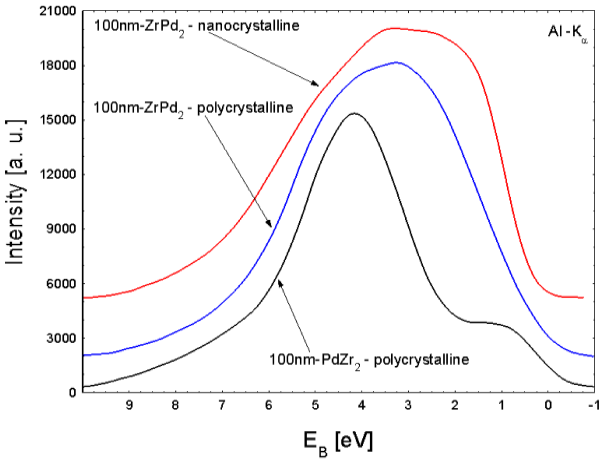

Fig. 3. XPS (Al-K$_\alpha$) valence band spectra for *in-situ* prepared nanocrystalline and polycrystalline $ZrPd_2$ thin films. For a comparison we show valence band spectrum of polycrystalline $PdZr_2$ thin film.

the same. On the other hand, the XPS valence band for polycrystalline $PdZr_2$ thin film is shifted due to significantly different composition. Furthermore, valence band measured for the nanocrystalline $ZrPd_2$ is considerably broadened compared to that measured for the polycrystalline sample. The above effect could be explained by a strong deformation of the nanocrystals [15–17]. For such nanocrystalline samples the interior of the nanocrystal is constrained and the distances between atoms located at the grain boundaries are expanded.

The XPS valence band measured for polycrystalline thin film was compared with the theoretical XPS valence bands determined from *ab initio* calculations for single crystal with chemical disorder (Fig. 4). The average grain size measured for the polycrystalline $ZrPd_2$ thin film was

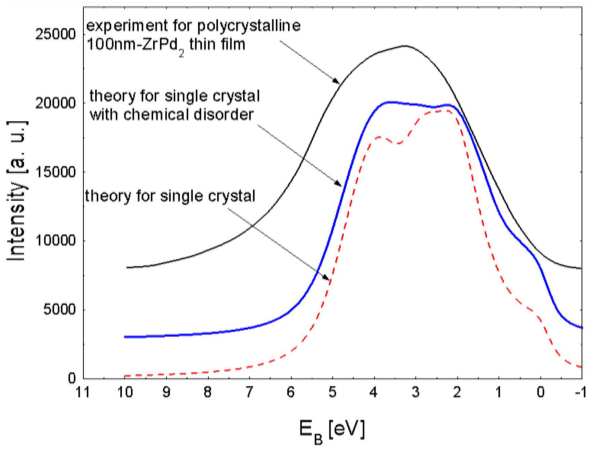

Fig. 4. Theoretical XPS valence bands for ideal single crystal $ZrPd_2$ and single crystal with chemical disorder as shown in Fig. 1. Both calculations are made in GGA+U, with U(Zr) = 2.4 eV and U(Pd) = 3.7 eV. For a comparison experimental XPS valence band measured for polycrystalline $ZrPd_2$ thin film.

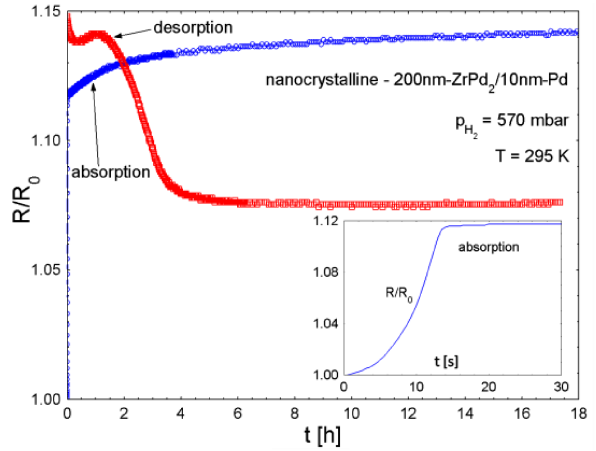

Fig. 5. Absorption and desorption kinetics for nanocrystalline $ZrPd_2$ thin film under a hydrogen pressure of 570 mbar.

estimated as about 100 nm [23]. The two features near –2.5 and –3.8 eV observed in the theoretical XPS valence band calculated for ideal single crystal are not detected in the experimental valence band data measured for the polycrystalline sample (see Fig. 4). This is probably as a result of stresses and grain boundaries in real polycrystalline alloy thin film.

In Fig. 5 we show relative resistivity change of the nanocrystalline 100 nm – $ZrPd_2$ alloy thin film during hydrogen absorption and desorption at a pressure of about 570 mbar. Note that immediately after preparation the alloy thin film was covered *in-situ* by 10 nm Pd layer to catalyze hydrogen absorption and to protect against oxidation. The sample shows rather fast resistivity change during the first 12 s of RT absorption (see inset in Fig. 5).

On the other hand, the polycrystalline 100 nm - $ZrPd_2$ covered by 10 nm of Pd showed practically no hydrogen absorption (resistivity change). The relatively fast absorption of hydrogen could be interesting in potential application of nanocrystalline $ZrPd_2$ as a membrane for industrial hydrogen purification, in good agreement with recent theory [10].

In conclusions, the different microstructures observed in poly- and nanocrystalline $ZrPd_2$ alloy thin films lead to significant modifications of their valence bands. Therefore, the nanocrystalline $ZrPd_2$ can absorb hydrogen even below 1 bar at RT. Nanocrystalline $ZrPd_2$ thin film materials could find potential application as a membrane for industrial hydrogen purification.

Acknowledgments

One of the authors (S.P.) would like to thank the Ministry of Science and Higher Education in Poland for financial support within the research project “Diamond grant”, 2015-19, No. DI2014010344.

References

[1] M. Gupta, A.R.P. Gupta, D.J. Singh, *Phys. Rev. Lett.* **95**, 056403 (2005).

[2] M. Ohring, *The Materials Science of Thin Films* Academic Press, San Diego 1991.

[3] W. D. Nix, *Metall. Trans. A* **20**, 2217 (1989)

[4] L. Smardz, M. Nowak, M. Jurczyk, *Int. J. of Hydrogen Energy* **37**, 3659 (2012).

[5] L. Smardz, M. Jurczyk, K. Smardz, M. Nowak, M. Makowiecka, I. Okońska, *Renewable Energy* **33**, 201 (2008).

[6] A. Pundt, C. Sachs, M. Winter, M. T. Reetz, D. Fritsch, R. Kirchheim, *J. All. Comp.* **293-295**, 480 (1999).

[7] J. W. Phair, R. Donelson, *Ind. Eng. Chem. Res.* **45**, 5657 (2006).

[8] N.W. Ockwing, T.M. Nenoff, *Chem. Rev.* **107**, 4078 (2007).

[9] M. D. Dolan, *J. Membr. Sci.* **362**, 12 (2010).

[10] N. Chandrasekhar, D.S. Sholl, *Journal of Membrane Science* **453**, 516 (2014).

[11] L. Smardz, *J. Alloys Comp.* **395**, 17 (2005).

[12] L. Smardz, K. Smardz, H. Niedoba, *J. Magn. Magn. Mater.* **220**, 175 (2000).

[13] L. Smardz, U. Köbler, W. Zinn, *Vacuum* **42**, 283 (1991).

[14] J. Skoryna, A. Marczyńska, L. Smardz, *J. Alloys Comp.* **645**, S384 (2015).

[15] K. Smardz, L. Smardz, I. Okonska, M. Nowak, M. Jurczyk, *Int. J. Hydrog. Energy* **33**, 387 (2008).

[16] L. Smardz, K. Smardz, M. Jurczyk, J. Jakubowicz, *J. All. Comp.* **313**, 192 (2000).

[17] M. Jurczyk, L. Smardz, M. Makowiecka, E. Jankowska, K. Smardz, *J. Phys. Chem. Sol.* **65**, 545 (2004).

[18] P. Blaha, K. Schwarz, G. Madsen, D. Kvasnicka, J. Luitz, *WIEN2k, An Augmented Plane Wave + Local Orbitals Program for Calculating Crystal Properties*, Ed. K. Schwarz, Techn. Universität Wien, Austria, (2001).

[19] A.P. Pikul, D. Kaczorowski, Z. Gajek, J. Stępień-Damm, A. Ślebarski, M. Werwiński, A. Szajek, *Phys. Rev. B* **81**, 174408 (2010).

[20] J.P. Perdew, K. Burke, M. Ernzerhof, *Phys. Rev. Lett.* **77**, 3865 (1996).

[21] E. Şaşoğlu, C. Friedrich, S. Blügel, *Phys. Rev. B* **83**, 121101 (2011).

[22] I. Jacob, O. Beeri, E. Elish, *J. All. Comp.* **221**, 129 (1995).

[23] J. Skoryna, S. Pacanowski, A. Marczyńska, M. Werwiński, Ł. Majchrzycki, A. Rogowska, M. Wachowiak, R. Czajka, L. Smardz, *Surf. Coat. Techn.* **303**, 125 (2016).